

PASSIVE MICROFLUIDIC MIXER FABRICATION AND FLOW TEST

A Thesis

Presented to the Faculty of the Graduate School

of Cornell University

In Partial Fulfillment of the Requirements for the Degree of

Master of Science

by

Yizui Yu

August 2012

© 2012 Yizui Yu

ABSTRACT

This study proposed different materials of microfluidic mixer fabrication and their flow test. Two different design based on a T-mixer were fabricated. J-shaped and vertical pillar micromixers were fabricated with Zeonor, PDMS, silicon and SU-8. Several methods were used to seal mixer and test the sealing effect. Using Cy5 and fluorescein to measure the mixing time of micromixer. The mixing results shows that the J-shaped micromixer has a good mixing function and a short mixing time.

BIOGRAPHICAL SKETCH

Yizui Yu earned his bachelor of Applied Physics degree in China from Beihang University in 2010. In 2010 he joined the M.S program in Cornell University. While pursuing his degree, Yizui Yu worked as a member of Lois group in Cornell University.

ACKNOWLEDGMENTS

The quality of this experiment was greatly enhanced by my advisor Lois Pollack. Thanks also to Christopher Jones, Steve Meisburger, Suzette A. Pabit. This work was also supported by the CNF.

TABLE OF CONTENTS

1. Introduction	1
1.1 Reynolds number	9
1.2 Mathematical model	12
1.3 Determination of mixing efficiency	13
2 Fabrication method	15
3. Device design	16
4. Fabrication	19
5. Flow test and confocal result	40
J-shaped mixer confocal flow test	43
Pillars mixer confocal flow test	53
6. Calculation	55
7 Conclusions	57
REFERENCES	59

1.

Introduction

Miniaturization is a current trend in analytical chemistry and life science. In the past two decades, microfluidic systems have attracted major research interest due to their promising potential for applications in biotechnology. Microfluidic applications include micro arrays, DNA sequencing, sample preparation and analysis, cell separation and detection, as well as environmental monitoring. Microfluidic devices, such as micropumps, microvalves, microsensors and micromixers have been developed in rapid succession in recent years (Shoji and Esashi, 1994). These devices attract interest from both industry and academia, because of their potential and advantages: small amounts of sample and reagent, rapid reaction, low cost and high throughput.

The micromixer is one important member of the microfluidic family. Until recently, the importance of micromixers was not well recognized thus only a few research groups were focused on this area. An early review on micromixers was provided by Kakuta et al [1]. Some general review papers on micro total analysis systems (microTAS) by Reyes et al [2], Vilkner et al [3] and Erbacher et al [4] also dealt briefly with micromixer. More recently, this kind of device attracted more research interest and a number of new micromixers have been introduced in research journals. Micromixers are widely used in chemical, biological and medical analysis fields. Almost every chemical assay requires mixing reagents with samples. The basic T-mixer was used for the measurement of analyte concentrations of a continuous flow. The micromixer reported by Hinsmann et al [5] was used for the study for rapid

chemical reactions in solution with stopped-flow, using time resolved Fourier transform infrared spectroscopy (TR-FTIR) for detection. Micromixers also can be used as sensors in environmental monitoring such as the detection of ammonia in aqueous solutions [6]. The fast mixing time of a micromixer benefits time-resolved measurement of reaction kinetics using nuclear magnetic resonance (NMR) [7]. Fast mixing with a micromixer was used in the freeze quenching technique, which is useful for trapping meta-stable intermediate populated during fast chemical or biochemical reaction [8]. Micromixers were also used for the sample preparation of a surface-based biosensor. Besides sensing and analysis application, micromixers were used as a tool for dispersing immiscible liquids and forming micro droplets [9]. Furthermore, micromixers work as a separator for particles based on their different diffusion coefficients or as a generator of concentration gradients [10].

Rapid and effective mixing is the basic requirement for a successful micromixer. Many microfluidic devices for improved mixing on the microscale have been fabricated. Generally mixing occurs in two ways in these devices: one is a heterogeneous mixing created by convection, and the other is a heterogeneous mixing at the molecular level caused by diffusion between adjacent domain [11]. It was noticed that sharp corners in a zigzag channel caused complete mixing due to turbulent flow in mini channels while in micro channels mixing was caused by diffusion only (Branebjerg et al., 1994). At the microscale rapid mixing is not produced by turbulence due to the extremely weak inertial forces. Therefore, one must employ a different mechanism to improve mixing in a micro system.

In general, micromixers can be divided into passive micromixers and active micromixers (figure 1). Two basic principles are followed to induce mixing at the microscale. First, energy input from the exterior is used, termed active mixing. Second, the flow energy, e.g. due to pumping action or hydrostatic potential, is used to restructure a flow in a way which results in faster mixing. This is known as passive mixing. Passive micromixers also can be categorized by the arrangement of the mixed phases: parallel lamination, serial lamination, injection, chaotic advection and droplet. Active micromixers need an external field for the mixing process. The different types of external influences effects such as pressure, temperature, electrohydrodynamics, dielectrophoretics, electrokinetics, magnetohydrodynamics and acoustics make different active micromixers. With the extra field, the structures of active micromixers are often complicated and require complex fabrication processes. In contrast, passive micromixers do not need external actuators except those for fluid delivery so that the structure and the fabrication process of passive micromixers are usually simple.

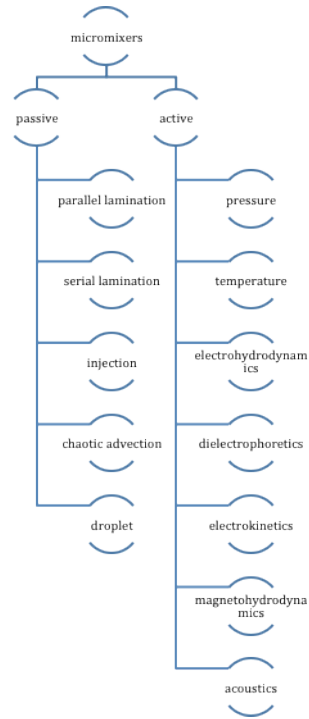


Figure 1. Classification scheme for micromixers

Passive micromixers

Because of its simple concept, the passive mixer was one of the first microfluidic devices reported. Due to the dominance of laminar flow on the microscale, mixing in passive micromixer relies mainly on molecular and chaotic advection. Designs for passive micromixers can range from a simple one such as tee mixer to more complex structures that aim to induce chaotic advection. Increasing the contact surface between the different fluids and decreasing the diffusion path between them could enhance molecular diffusion. Chaotic advection can be realized by manipulating the laminar flow in microchannels. The resulting flow pattern decreases the diffusion path, increasing the mixing efficiency.

Lamination mixer

As a basic design, the Tee mixer is ideal for investigations of passive micromixer. It consists of two inlet ports through which the two different fluids are injected, and one outlet channel where the mixing of the two different fluids occurs. Since the basic T-mixer entirely depends on molecular diffusion, a long mixing channel is needed. If run at an extremely high Reynolds number mixing could also occur in a short channel because efficient mixing in a simple T-mixer requires very high Reynolds numbers. However, several improvements have made to T-mixer design to increase mixing efficiency. In the work of Yi and Bau [12], a Y-mixer made of co-fired ceramic tapes with a 90° bend can generate vortices at Reynolds numbers above 10. At Reynolds numbers higher than 30, mixing is achieved right after the bend.

Improving the efficiency of mixing is one of the most important targets to design a new micromixer. A simple method is reducing the mixing path to improve the mixing efficiency. The basic idea is making a narrow mixing channel to realize parallel lamination with multiple streams. One concept for reducing mixing path for parallel lamination micromixers is hydrodynamic focusing [13]. The basic design for hydrodynamic focusing is a long microchannel with three inlets. Fluid flows on two channels pushes on flow to the third. This hydrodynamic focusing reduces the stream width of the third channel, and consequently the mixing path. Pollack lab also introduced a five-inlet port mixer for investigations of rapid kinetic reactions involving biological macromolecules [14].

Chaotic advection mixer

In a passive micromixer, as we mention before, the mixing process relies on diffusion and chaotic advection. Advection is often parallel to the main flow direction, and is not useful for the transverse mixing process when reagents are co-flowing in parallel streams. However, chaotic advection is much more important than diffusion in flows with low Reynolds number. The so-called chaotic advection can improve mixing significantly. Generally, chaotic advection can be generated by the use of special geometries in the mixing channel or induced by an external force. While the former is a passive micromixer, the latter is an active micromixer. For a passive micromixer to realize chaotic advection, the channel shape can be modified for splitting, stretching, folding and breaking of the flow. The simplest method to achieve chaotic advection with a high Reynolds number is to insert obstacles structures in the mixing channel. These obstacles could alter the flow directions and force fluids to merge and create transverse mass transport. Another method to generate chaotic advection is using zig-zag microchannels to produce recirculation around the turns at high Reynolds numbers. However, realizing a chaotic advection with a low Reynolds number is not so easy. Johnson et al [15] were the first to investigate the rips or grooves on the channel wall that can produce chaotic advection.

As we mention before, passive micromixers can be categorized into parallel lamination, serial lamination, injection, chaotic advection, and droplet. The basic T-mixer and Y-mixer geometric are parallel lamination micromixers. Serial lamination

micromixers are similar to parallel lamination micromixers. Serial lamination micromixers enhance mixing through splitting and later rejoining the streams. The mixers reported by Branbjerg et al [16] Schwesinger et al [17] were fabricated in silicon using the wet etching in KOH or deep reactive ion etching (DRIE) technique. The concept of the injection mixer is also similar to the parallel lamination mixer. Instead of splitting both inlet flows, this kind of mixer only splits the solute flow into many streams and injects them into the solvent flow. On top of one stream is an array of nozzles, which create a number of microplumes of the solute. These plumes increase the contact surface and decrease the mixing path. Mixing efficiency can be improved significantly. Forming droplets of the mixed liquids is another solution for reducing the mixing path. The movement of a droplet causes an internal flow field and makes mixing inside the droplet possible. In general, droplets can be generated and transported individually using pressure or capillary effects such as thermo capillary and electrowetting. Furthermore, droplets can be generated due to the large difference of surface forces in a small channel with multiple immiscible phases such as oil/water or water/gas.

Active micromixers

Due to the low Reynolds number associated with microscale fluid flow, it is difficult to rapidly and homogeneously mix two fluids in a passive micromixer. Active micromixers, fast and homogenized mixing devices, seem to be a better choice. Pressure field disturbances were used in one of the earliest active micromixers.

Deshmukh et al [18] reported a T-mixer with pressure disturbance. This mixer is integrated in a microfluidic system, which is fabricated in silicon using DRIE. In addition to pressure disturbance, a structure of a micromixer with electrohydrodynamic disturbance is reported by Niu and Lee [19]. Instead of pressure sources, electrodes are placed along the mixing channel. Dielectrophoretic flow can be used in an active micromixer. Dielectrophoresis (DEP) is the polarization of a particle relatively to its surrounding medium in a non-uniform electrical field. This effect causes the particle to move to and from an electrode. Deval et al and Lee et al reported a dielectrophoretic micromixer [20]. Chaotic advection was generated by embedded particles with a combination of an electrical actuation and local geometry channel variation. Electrokinetic flow also can be used to transport liquid in micromixers as an alternative to pressure-driven flow. Jacobson et al [21] reported electrokinetically driven mixing in a conventional T-mixer. Tang et al also utilized an electrokinetic flow to improve mixing [22]. The magneto hydrodynamic effect has also been used in micromixers. In the presence of an external magnetic field applied dc voltages on the electrodes generate Lorentz forces, which in turn induce mixing movement in the chamber. The Lorentz force can roll and fold the liquid in a mixing chamber. This kind of mixer was reported by Bau et al [23]. It was fabricated from co-fired ceramic tapes and the electrodes are printed with gold paste. Acoustic actuators were used to stir fluids in micromixers. The proof of concept for acoustic mixing was reported by Moroney et al [24] with a flexible-plate-wave (FPW) device. Zhu and Kim [25] gave an analysis of the focused acoustic wave model in a mixing chamber and made an

acoustic micromixer with silicon. However, since the diffusion coefficient also depends highly on temperature, the thermal energy can be used to enhance mixing. Mao et al [26] generated a linear temperature gradient across a number of parallel channels in order to investigate the temperature dependence of fluorescent dyes. However, several other mixing concepts also have been presented. Woias et al. at the Fraunhofer-Institute for Integrated Circuit and System have presented a micromixer using a silicon chip with a thin piezoelectrically actuated membrane [27]. This micromixer comprises a piezoelectric membrane actuator, a wide cavity, two fluid inlets, and an outlet. The feasibility of the mixer was demonstrated with colorimetric pH detection showing relatively slow mixing but high repeatability. Yasuda from the Department of Life Science at the University of Tokyo realized the production of a micromixer using acoustic radiation force [28]. Hosokawa et al. from the Mechanical Engineering Laboratory at AIST/MITI have presented a microfluidic device for active pneumatic mixing of two liquid droplets [29].

1.1 Reynolds number

In fluid mechanics, the Reynolds number (Re) is a dimensionless number that gives a measure of the ratio of inertial forces to viscous forces and consequently quantifies the relative importance of these two types of forces for given flow condition. The concept was introduced by George Gabriel Stokes in 1851 [30], but the Reynolds number is named after Osborne Reynolds (1842-1912).

The Reynolds number can be obtained when one uses the nondimensional form of the incompressible Navier-Stokes equations:

$$\rho \left(\frac{\partial V}{\partial t} + V \cdot \nabla V \right) = -\nabla p + \mu \nabla^2 V + f$$

Each term in the above equation depends on the exact measurements of a flow.

The Reynolds number also can be defined for a number of different situations where a fluid is in motion relative to a surface. These definitions generally include the fluid properties of density and viscosity, plus a velocity and a characteristic length or characteristic dimension. This dimension is a matter of convention – for example a radius or diameter is equally valid for spheres or circles, but one is chosen by convention. For aircraft or ships, the length or width can be used. For flow in a pipe or a sphere moving in a fluid the internal diameter is generally used today.

$$Re = \frac{\rho v L}{\mu} = \frac{v L}{\nu}$$

Where:

v is the mean velocity of the object relative to the fluid (unit: m/s)

L is a characteristic linear dimension (unit: m)

μ is the dynamic viscosity of the fluid (unit: Pa•s or N•s/m² or kg/(m•s))

ν is the kinematic viscosity (unit: m²/s)

ρ is the density of the fluid (unit: kg/m³)

For flow in a pipe or tube, the Reynolds number is generally defined as:

$$Re = \frac{\rho v D_H}{\mu} = \frac{v D_H}{\nu} = \frac{Q D_H}{\nu A} \quad [31]$$

Where:

D_H is the hydraulic diameter of the pipe (unit: m)

Q is the volumetric flow rate (unit: m^3/s)

A is the pipe cross-sectional area (unit: m^2)

V is the mean velocity of the object relative to the fluid (unit: m/s)

μ is the dynamic viscosity of the fluid (unit: Pa•s or N•s/ m^2 or kg/(m•s))

ν is the kinematic viscosity (unit: m^2/s)

ρ is the density of the fluid (unit: kg/ m^3)

For shapes such as squares, rectangular or annular ducts where the height and width are comparable, the characteristic dimension for internal flow situation is taken to be the hydraulic diameter, D_H , defined as:

$$D_H = \frac{4A}{P}$$

where A is the cross-sectional area and P is the wetted perimeter. The wetted perimeter for a channel is the total perimeter of all channel walls that are in contact with flow [32]. This means the length of the water exposed to air is not included in the wetted perimeter.

For a circular pipe, the hydraulic diameter is exactly equal to the inside pipe diameter, as can be shown mathematically.

For an annular duct, such as the outer channel in a tube-in-tube heat exchanger, the hydraulic diameter can be shown algebraically to reduce to:

$$D_{H, \text{annular}} = D_o - D_i$$

where:

D_o is the inside diameter of the outside pipe

D_i is the outside diameter of the inside pipe

For calculations involving flow in non-circular ducts, the hydraulic diameter can be substituted for the diameter of a circular duct, with reasonable accuracy.

1.2 Mathematical model

Compared with an active micromixer, the mathematical model of passive micromixer is much simpler, especially the T-mixer. The equations used to describe the system are continuity, Navier-Stokes (pressure and velocity) and the species convection-diffusion equations. Derivations and details of the equations can be found in Bird et al [33], and their dimensionless forms are shown in below equations:

$$\nabla \cdot v = 0$$

$$\frac{\partial v}{\partial t} = -\nabla p + \frac{1}{Re} \nabla^2 v$$

$$\frac{\partial x_a}{\partial t} = \frac{1}{ReSc} \nabla^2 x_a$$

where

$$Re = \frac{\rho u d}{\mu}$$

$$Sc = \frac{\mu}{\rho D_{ab}}$$

a is the species a

b is the species b

v is the velocity vector

x is the mole fraction

t is the time

p is the pressure

$D_{a,b}$ is the diffusion coefficient of a in b

A physical description can be assigned to the above dimensionless groups. The Reynolds number (Re) characterizes the ratio of the inertial to the viscous forces. The product of the Schmidt number (Sc) and the Reynolds number describes the ratio of mass transport by convection to that by diffusion. This product is termed the Peclet number (Pe) and is given by $(ud/D_{a,b})$.

1.3 Determination of mixing efficiency

The most common and simplest way to evaluate mixing in micromixer structures is by flow visualization via dilution-type experiments usually with the aid of microscopic-, photo-, video- or high-speed camera techniques. This is done by contacting dyed and transparent liquid streams (passive mixing) or standing volumes (active mixing) in a type of photometric experiment. In fluorescence experiments, visualization is achieved

by fluorescent streams; in a commonly applied reaction variant, mixing is allocated by monitoring quenching of fluorescent stream.

Reaction-type experiment underlay the mixing with a very fast reaction so that mixed regions spontaneously indicate the result of the reaction. The simplest outcome of a reaction is the formation of a colored species such as observed by the iron rhodanide reaction. Acid- base reactions with a pH-sensitive dye are also extremely fast reactions that spontaneously induce color changes. Depending on the time required for reaching the mixed state, the ratio of the products of the competing reactions can considerably differ as a consequence of different reaction environments (pH, solvent, etc.) and be used as a measurement of mixing efficiency.

Another frequently applied competitive approach for the characterization of micromixer devices is the Dushman reaction, by which iodine is formed via an acid catalyzed redox reaction between iodine and iodate. This reaction was first applied for determining mixing efficiency in stirred batch reactors and then adapted to the needs of micromixer devices. Later, an optimized protocol was developed for the Dushman reaction giving more accurate and better reproducible results.

Concentration profiling uses on or inline measurements of optical properties, typically not done for the whole volume, but along lines such as the projected channel cross-section. Measuring several cross-sectional profiles at varying distance in a flow-through mixing channel gives the temporal evolution of the mixing using detailed spatial information. Concentrations are accessible by photometric or fluorescence measurements. Electrode based concentration detection is used as well.

Besides using photometric techniques, vibrational analysis such as IR and Raman can be used for following the mixing course in a micromixer device. Using an IR microscope, FTIR spectra at various channel sites can easily be monitored, if an IR-transparent construction material such as silicon is used.

2 Fabrication method

A variety of fabrication techniques have been used for making micromixers. The different techniques can be categorized as silicon micromachining and polymeric micromachining.

Most of the early micromixers were made of silicon. The mixing channels were either wet etched with KOH or dry etched using deep reactive ion etching (DRIE). A glass cover is anodically bonded on top of the channel offering both sealing and optical access. Passive micromixers can be made entirely of glass. In some applications such as mixing of electrokinetic flows, silicon cannot be used because of its electrically conducting properties. Most active micromixers with integrated actuators are fabricated in silicon because of established technologies such as sputtering of metals and piezoelectric materials.

Besides the advantages of an established technology, silicon-based micromixers are relatively expensive because of the large surface needed for microchannels and the clean room conditions for fabrication. On the other hand, silicon devices are not always chemically and biochemically compatible. Polymeric micromachining offers a lower fabrication cost and a faster prototyping cycle. A simple approach established

by Whiteside's group [34] at Harvard University has been repeated recently by many other groups. This low cost approach uses a lithography mask printed from a high-resolution laser printer. The mask is then used for the subsequent photolithography of the thick film negative photoresist SU-8 on a silicon wafer. The silicon wafer works as a mold for an elastomer such as polydimethylsiloxane (PDMS) or zeonor.

The thick film photoresist SU-8 can be used directly for making micromixers. SU-8 microchannels are formed on a silicon or glass substrate. SU-8 has the advantage of simple micromachining. Moveable structures such as microvalves and microgrippers have been fabricated with the so-called polymeric surface micromachining. This approach proves the feasibility of making a complex microfluidic system with moveable structures in SU-8.

Mixing channels can also be fabricated by hot embossing with a hard template, which can be micromachined in silicon, glass, or metals such as nickel [35]. This approach is limited to a 2-dimensional channel structure but promises a simple method for mass production. Faster prototyping can be achieved with laser micromachining of thin polymer and adhesive sheets [36]. However, the resolution of this approach is limited by the wavelength of the laser.

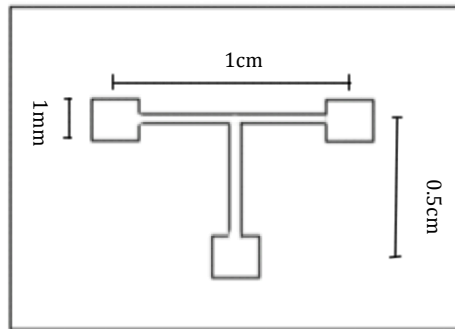
3. Device design

The tee passive micromixer is a well-known device for a simple mixer. It consists of two inlet ports through which the two different fluids are injected, and one outlet

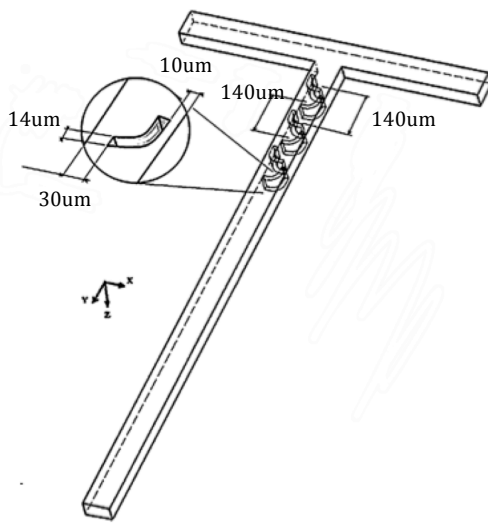
channel where the mixing of the different fluids occurs. Mixing occurs within such a device but can be slow. Two alternate designs with improved mixing forms are discussed below.

3.1 J-shaped passive micromixer

The cross section of the microchannel (Fig.2) measures $100\mu\text{m} \times 50\mu\text{m}$, and the length of the main channel is 0.5 cm. In order to enhance the mixing of the two fluids, J-shaped baffles are employed, as shown in Fig. 2 (a). They induce lateral convection in the main channel. The $14\mu\text{m}$ high J-shaped baffles are located at $10\mu\text{m}$ and $30\mu\text{m}$ from either side of the channel, as illustrated in the figure.



(a)



(b)

Figure. 2 Schematic diagram of (a) T-mixer, and (b) T-mixer with seven J-shaped baffles in the main channel

3.2 Passive micromixer with vertical pillars

The top view of the mixing chamber is shown in Fig. 3. The two solutions flow head to head through a $50\mu\text{m}$ wide channel prior to entering the $50\mu\text{m} \times 100\mu\text{m}$ mixing chamber that is arranged in a T geometry. Within the mixing chamber, seven $10\mu\text{m}$ diameter vertical pillars are arranged perpendicular to the flow direction and in a staggered fashion.

Both types devices of mixing device were fabricated.

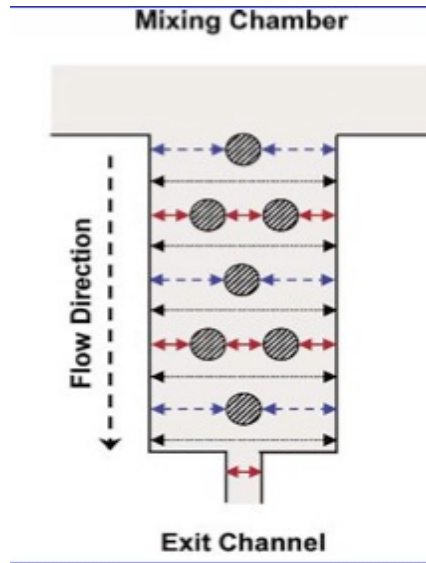


Figure 3. A schematic of T-mixer with seven pillars. The alternating 10, 20 and 50 μ m passages along the flow direction are indicated by the solid, dashed, and dotted double arrows.

4. Fabrication

4.1 Material

Four different materials were used to fabricate these two designs: zeonor, polydimethylsiloxane (PDMS), silicon and SU-8.

Zeonor

Zeonor is widely used in various medical applications because of its great properties.

Zeonor is a line of thermoplastic polyolefin resin with an excellent combination of

optical and electronic properties. It is a one kind of Cyclic Olefin Polymers (COP) similar to Zeonex. Zeonor offers many great properties and is: a high transparency- 92% in visible range 400-800nm, a low fluorescence-less than PC or PS, a low water absorption-less than 0.01%per 24hours and a good chemical resistance. Zeonor® 1060R Cyclo Olefin Polymer was used in this experiment.

PDMS

Polydimethylsiloxane (PDMS) belongs to a group of polymetric organosilicon compounds that are commonly referred to as silicones [37]. The chemical formula for PDMS is $\text{CH}_3[\text{Si}(\text{CH}_3)_2\text{O}]_n\text{Si}(\text{CH}_3)_3$, where n is the number of repeating $[\text{Si}(\text{CH}_3)_2\text{O}]$ monomer units. Depending on the size of the string of monomer, the non-cross-linked PDMS may be almost liquid (poor n) or semi-solid (large n). PDMS is the most widely used silicon-based organic polymer. It is particularly known for its unusual rheological (or flow) properties. PDMS is optically clear, and, in general, is considered to be inert, non-toxic and non-flammable. PDMS is viscoelastic, meaning that at long flow times (or high temperatures), it acts like a viscous liquid, similar to honey. However, at short flow times (or low temperature), it acts like an elastic solid, similar to rubber. After polymerization and cross-linking, solid PDMS samples will present an external hydrophobic surface [38]. This surface chemistry makes it difficult for polar solvents (such as water) to wet the PDMS surface, and may lead to adsorption of hydrophobic contaminants. Plasma oxidation can be used to alter the surface chemistry, by

adding silanol (SiOH) groups to the surface. This treatment renders the PDMS surface hydrophilic, allowing water to wet (this is frequently required for water-based microfluidics). The oxidized surface resists adsorption of hydrophobic and negatively charged species. The oxidized surface can be further functionalized by reaction with trichlorosilanes. Oxidized surfaces are stable for about 30 minutes in air, afterward hydrophobic recovery of the surface is inevitable independent of whether the surrounding medium is vacuum, air or water.

Silicon

Silicon is the eighth most common element in the universe by mass, but very rarely occurs as a pure free element in nature. It is most widely distributed in dusts, sand, planetoids and planets as various forms of silicon dioxide (silica) or silicates. Over 90% of the Earth's crust is composed of silicate minerals, making silicon the second most abundant element in the earth's crust (about 28% by mass) after oxygen. In electronics, a wafer (also called a slice or substrate) is a thin slice of semiconductor material, such as a silicon crystal, used in the fabrication of integrated circuits and other microdevices. Wafers are manufactured from highly pure (99.9999999% purity) [39], nearly defect-free single crystalline material. One process for forming crystalline wafers is known as Czochralski growth invented by the Polish chemist Jan Czochralski [40]. In this process, a cylindrical ingot of high purity monocrystalline silicon is formed by pulling a seed crystal from a 'melt' [41]. Dopant impurity atoms such as boron or

phosphorus can be added to the molten intrinsic silicon in precise amounts, thus changing it into n-type or p-type extrinsic silicon. The ingot is then sliced with a wafer saw (wire saw) and polished to form wafers.

SU-8

SU-8 is a commonly used epoxy-based negative photoresist. It is a very viscous polymer that can be spun or spread, yielding a film with a thickness ranging from <1 micrometer up to >300 micrometer. This film can be processed with standard contact lithography. It can be used to pattern high aspect ratio (>20) structures. [42] Its maximum absorption occurs for ultraviolet light with a wavelength of 365nm (it is not practical to expose SU-8 with g-line ultraviolet light). When exposed, SU-8's long molecular chains cross-link causing the solidification of the material. SU-8 was originally developed as a photoresist for the microelectronics industry, to provide a high-resolution mask for fabrication of semiconductor devices. Because it is easy to pattern, it is now mainly used in the fabrication of microfluidics (mainly via soft lithography, but also with other imprinting technique such as nanoimprint lithography [43]) and microelectromechanical systems parts. It is also one of the most biocompatible materials known and is often used in bio-MEMS.

4.2 Experimental setup

Four different methods were used to fabricate passive micromixers, however the setup of fabricating mask is the same for all.

4.2.1 Fabrication

L-edit 15 is used to design our mask. For zeonor and PDMS devices, the mask yields 2 J-shaped mixers and 2 vertical pillars mixers. For silicon devices we made 16 vertical pillars mixers in a single mask. We use a PG mask writer to make our mask. This writer is a laser interferometer metered pattern generator for patterns on chrome mask blanks. Its vacuum plateholder accommodates 2-inch through 7-inch plates with a standard mask thickness of 0.090 inch. The range of feature size is $2\mu\text{m}$ to 1.5mm in $0.5\mu\text{m}$ increments and aperture rotation is from 0° through 89.9 degrees in 0.1-degree increments. With a $0.1\mu\text{m}$ grid data input, exposed images can be positioned with $0.6\mu\text{m}$ accuracy in each coordinate over the full 150mm of stage motion. When used with the 5X or 10X GCA stepper, this instrument is almost always sufficient for mask making. The files from L-edit 15 were transferred to GDS files and then transferred to PG mask writer. 5X stepper and layer 1 were used. The process usually takes 90mins with 7000 exposures. After writing, the mask is loaded into the Hamatech Mask Plate Processor with the resist side up. This processor is an automatic system for mask developing and etching. After developing and etching, the resist stripping deck in the photolithography room is used to remove resist. Usually the mask will stay in the right

strip tank (AZ 300T) for 10mins and then in the left strip tank (AZ 300T) for 10mins. After resist stripping, the mask transferred to the dump rinse tank and spin rinse dryer.

4.2.2 Master fabrication for zeonor and PDMS

YES Vapor Prime Oven is used for wafer preparation. The YES LP-III is a vacuum oven that can be used for HMDS vapor priming. Using hexamethyldisilazane (HMDS), the unit functions as a standard vacuum vapor primer. Clean wafers are dehydrated through a series of heated (150C) evacuation and dry N₂ refills. HMDS vapor then evaporates into the evacuated chamber forming a monolayer on the wafer surfaces. Vapor priming is used to improve the adhesion of the photoresist to the wafer. The ABM contact aligner is used to expose our wafer. The ABM is a very versatile instrument with interchangeable light sources, which allow Near-UV (405-365nm) as well as Mid- and Deep-UV (254nm, 220nm) exposures in proximity (non-contact) or contact (soft & hard) modes. The exposure can cover an area 200 mm in diameter. The printing resolution is 0.8µm for Near-UV and 0.4µm for Mid-UV and Deep-UV in vacuum contact mode. In our experiments, the exposure time is 15sec and the minimum feature is 5µm wide.

A single chamber (licensed Bosch fluorine process) inductively coupled plasma / reactive ion etcher, Unaxis 770 Deep Si Etcher was used to etch wafers. The Unaxis SLR 770 etches deep patterns in single crystal silicon substrates. The resulting features are used for MEMS and biological applications. Etch rates of up to 2 microns per minute and aspect ratios of 20:1 can be obtained using photoresist or silicon dioxide as

a masking medium. The final master we fabricated in the Unaxis is $49.93\mu\text{m}$ deep and the minimum feature is $5\mu\text{m}$ wide.

4.2.3 Zeonor device

A hot Press is used to fabricate zeonor device. The CRC Hot Press in the CNF lab provides up to 1600 lb (7000N) at temperatures up to 200°C .

These are the recommended step for embossing a zeonor device:

1. Cut zeonor into small pieces ($1.5\text{cm} \times 1.5\text{cm}$ or bigger) and clean them with acetone, IPA and DI water, preferably using an ultrasonic bath. Then dry all chips under the clean bench and place the Si master, zeonor chips, and glass pieces in containers to prevent getting dust on them.
2. Before starting, preheat the hot plate to 90°C . Clean the Si master, glass, and zeonor with nitrogen gun.
3. Set the Hot Press to 275 F (130°C top and 125°C bottom), 240 PSI for one device, 350 PSI for two devices, and 500 PSI for four devices. To apply force, press the two black buttons until the hot plates touch, and then adjust force. Wait until the temperature and force stabilize (roughly 20 minutes).
4. Stack the Si master (bottom), zeonor 1.5×1.5 chip (middle), glass piece (top), then place a folded beta wipe (pre-press folded wipe without master/chip sandwich to get permanent fold) such that all is centered. Then place this stack carefully between the Hot Press plates. Press the two black buttons until the pressure stabilizes, set timer for 10 minutes. (Use 4" square $1/4$ " thick

borosilicate glass for embossing 4 devices at once)

5. When done, remove the stack from the hot press and carefully place the wafer, zeonor and glass chip to cool on the hot plate. Lower hot plate temperature 10°C each 5 minutes. Lift off will happen automatically in 10-15 minutes. Peel apart gently.

4.2.4 PDMS device

PDMS should be mixed in a range from 1:5 to 1:20 ratio of curing agent and PDMS monomers. (1:10 is the ideal ratio). The PDMS monomers are much more viscous than the curing agents. For a 4-device wafer, usually a mixture, which consists of 4g of curing agent and 40g of monomer, will be used. The PDMS can be mixed in a disposable plastic cup. A wider cup may be better because it exposes a large surface of the contained fluid to air, which will aid in degassing the PDMS later. Place the 4-device wafer in a container and then pour the PDMS into container. Make sure that the wafer is totally immersed in PDMS, and then degas. The precise amount of time needed to fully degas the mixture will depend on the amount of PDMS being mixed and the width of the cup. Usually 1 hour is sufficient for full degassing. Once the PDMS has been degassed, remove it from the vacuum and place the container in the oven (set temperature at 70°C) for 4 hours or at room temperature for 24 hours. Most master breakages will occur during the unmolding process. It is important to be gentle when removing the PDMS from the master with small knife. Then separate the PDMS devices from the whole PDMS.

4.2.5 Master fabrication for silicon

To fabricate silicon device, the processing is the same as PDMS / zeonor device, except that negative photoresist (AZ nlof 2020 was used in our experiment) is used instead of positive photoresist (S1813). The spin speed is set to 2000rpm and spin time is 30 seconds. The Unaxis 700 Deep Si Etcher was also used for etching.

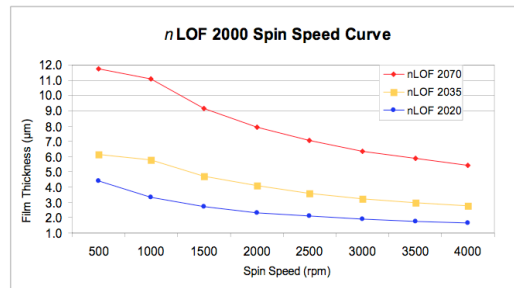


Figure 4. Spin speed curve of AZ nLOF 2000 photoresist

4.2.6 SU-8 device fabrication

The processing of fabricating SU-8 device has some differences from silicon device.

Two hours pre-bakes but no primer are needed for wafer preparation. For SU-8 2035, spin at 2000rpm for 30sec form films.

S1813 is used as our photoresist, the spin speed is 2000rpm and the spin time is 30sec.

After spinning, the wafer is baked at 115 °C for 60sec.

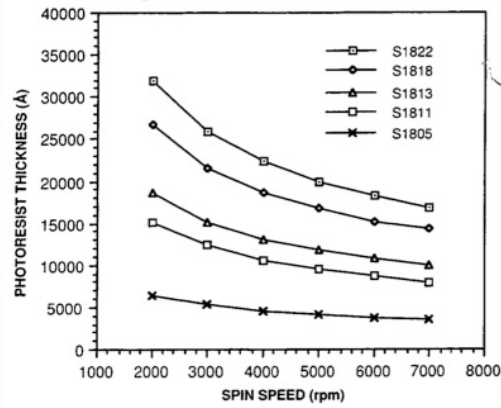


Figure 5. Spin speed curves of microposit S1800 photo resist undyed series

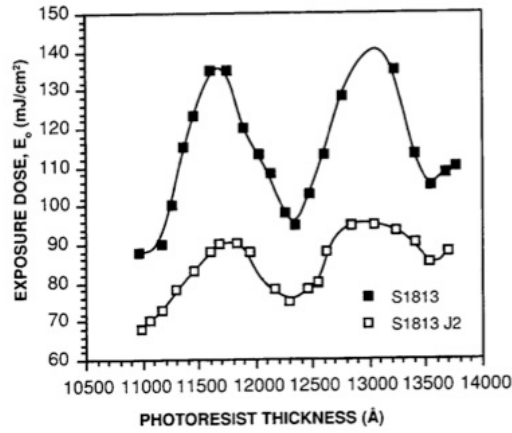


Figure 6. Interference curves of microposit S1813 and S1813 J2 photoresist

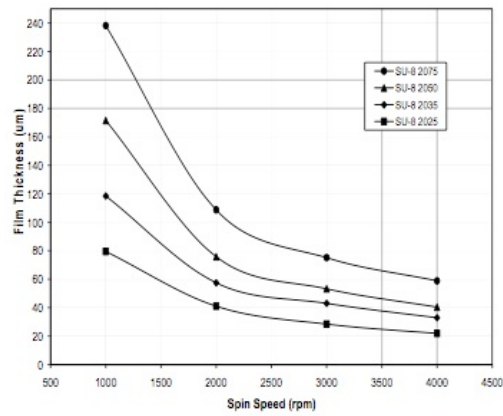


Figure 7. SU-8 2000 Spin Speed versus Thickness

Usually the thickness of SU-8 2035 with spin speed of 2000 rpm is between 40-60 μ m. The exact thickness will depend on the wafer preparation, pouring SU-8, pre-bake and post-bake.

Recommended program for SU-8 2035:

1. Dispense 1ml of resist for each inch (25mm) of substrate diameter.
2. Spin at 500 rpm for 5-10 seconds with acceleration of 100 rpm/second.
3. Spin at 2000 rpm for 30 seconds with acceleration of 300 rpm/second.

During the spin coat process step, photoresist may build up on the edge of the substrate. In order to minimize contamination of the hotplate, this thick bead should be removed. This can be accomplished using a small stream of solvent (MicroChem's EBR PG) at the edge of the wafer either at the top or from the bottom. Most automated spin coaters now have this feature and can be programmed to do this automatically. By removing any edge bead, the photomask can be placed into close contact with the wafer, resulting in improved resolution and aspect ratio.

A level hotplate with good thermal control and uniformity is recommended for use during the soft bake step of the process. Convection ovens are not recommended.

During convection oven baking, a skin may form on the resist. This skin can inhibit the evolution of solvent, resulting in incomplete drying of the film and/or extended bake times.

THICKNESS microns	SOFT BAKE TIMES	
	(65°C) minutes	(95°C) minutes
25 - 40	0 - 3	5 - 6
45 - 80	0 - 3	6 - 9
85 - 110	5	10 - 20
115 - 150	5	20 - 30
160 - 225	7	30 - 45

Table 1. SU-8 2035 soft bake temperature and times

To optimize the baking times/conditions, remove the wafer from the hotplate after the prescribed time and allow it to cool to room temperature. Then, return the wafer to the hotplate. If the film ‘wrinkles’, leave the wafer to the hotplate for a few more minutes. Repeat the cool-down and heat-up cycle until ‘wrinkles’ are no longer seen in the film. A long rest time between soft bake and exposure is not recommended for SU-8. To obtain vertical sidewalls in the SU-8 2035 resist, a long pass filter is used to eliminate UV radiation below 350 nm. A 365-LP filter is recommended for the ABM contact aligner. However, with the long pass filter, an increase in exposure time of approximately 40% is required to reach to the optimum exposure dose.

THICKNESS microns	EXPOSURE ENERGY mJ/cm ²
25 - 40	150 - 160
45 - 80	150 - 215
85 - 110	215 - 240
115 - 150	240 - 260
160 - 225	260 - 350

Table 2. SU-8 2035 exposure dose

RELATIVE DOSE	
Silicon	1X
Glass	1.5X
Pyrex	1.5X
Indium Tin Oxide	1.5X
Silicon Nitride	1.5 - 2X
Gold	1.5 - 2X
Aluminum	1.5 - 2X
Nickel Iron	1.5 - 2X
Copper	1.5 - 2X
Nickel	1.5 - 2X
Titanium	1.5 - 2X

Table 3. Exposure doses for various substrates

A post exposure bake should take place directly after exposure. No image will be seen before the post exposure bake on photomask. After 1 minute of post exposure bake at 95°C, an image of the mask should be visible in the SU-8 2035 photoresist coating. If no visible latent image is seen during or after post exposure bake this means that there was insufficient exposure, heating or both.

THICKNESS microns	PEB TIME (65°C)* minutes	PEB TIME (95°C) minutes
	25 - 40	1
45 - 80	1 - 2	6 - 7
85 - 110	2 - 5	8 - 10
115 - 150	5	10 - 12
160 - 225	5	12 - 15

* Optional step for stress reduction

Table 4. SU-8 2035 post exposure bake time

SU-8 2035 photoresist has been designed for use in immersion, spray or spray-puddle processes with MicroChem's SU-8 developer. Other solvent based developers such as ethyl lactate and diacetone alcohol may also be used. Strong agitation is recommended when developing high aspect ratio and/or thick film structures. The recommended development times for immersion processes are given in Table 5. However, the exact

development time depends on the design structure. Smaller features will require longer development time.

THICKNESS	DEVELOPMENT TIME
microns	minutes
25 - 40	4 - 5
45 - 75	5 - 7
80 - 110	7 - 10
115 - 150	10 - 15
160 - 225	15 - 17

Table 5. Development times for SU-8 developer

When using SU-8 developer, spray and wash the developed image with fresh solution for approximately 10 seconds, followed by a second spray/wash with Isopropyl Alcohol (IPA) for another 10 seconds. A white film produced during IPA rinse is an indication of underdevelopment of the unexposed photoresist. Simply immerse or spray the substrate with additional SU-8 developer to remove the white film and complete the development process. Air dry with filtered, pressurized air or nitrogen. SU-8 2035 has good mechanical properties. However, for applications where the imaged resist is to be left as part of the final device, a hard bake can be incorporated into the process. This is generally only required if all or part of the final device is to be subject to thermal processing during regular operation. A hard bake or final cure step is added to ensure that SU-8 2035 properties do not change in actual use. SU-8 2035 is a thermal resin and as such its properties can continue to change when exposed to a higher temperature than previously encountered. Using a final bake temperature 10°C higher than the maximum expected device-operating temperature is strongly

recommended. Depending on the degree of cure required, a bake temperature in the range of 150°C to 250°C for a time between 5 and 30 minutes is typically used. The hard bake step is also useful for annealing any surface cracks that may be evident after development. The recommended step is to bake at 150°C for a couple minutes. This applies to all film thickness.

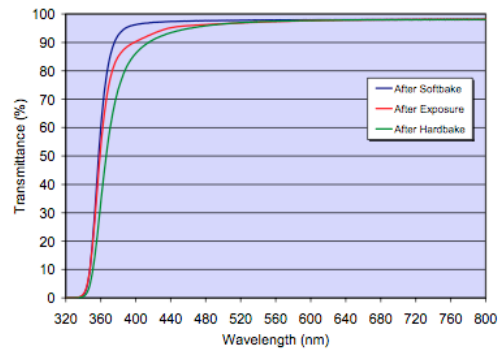


Figure 8. SU-8 2035 optical transmittance

4.3 Device sealing

With the processes we mention above, four different material devices are fabricated. Zeonor, silicon, SU-8, PDMS. Every material has several different sealing processes.

4.3.1 Zeonor

Before sealing zeonor devices, input and output holes should be drilled. High temperature was the first method used to seal the zeonor device. A blank zeonor chip

and a zeonor mixer were centered, and then placed into an oven at 95°C for 5 minutes. With these conditions, these two zeonor chips bond together. However, this mixer can not hold high pressure and falls apart easily. We also tried 115C for 10 minutes. At these conditions, the zeonor chip melts and distorts. Hot-press and plasma generator were also used after the failure with oven. A blank zeonor chip and a zeonor device were first oxidated in plasma generator and then put into a hot-press for 15 minutes. Hot-press was pre-set at 100C and 210lb. This method will have a good sealing between two zeonor chips and they do not separate. However it seems hot-press is not a good tool to seal zeonor device for flow experiments. High temperature and pressure will destroy small features in device. Most commonly the zeonor melts at high temperature and blocks the input channel.

RTV was the second method used to seal zeonor device. RTV is short for “room temperature vulcanizing”. RTV sealants are widely used in many different industrial sectors, from motor vehicle to electronic devices. There are two types of room temperature vulcanizing silicone: RTV-1 (one-component systems) and RTV-2 (two-component systems). In our sealing experiment, RTV-2 was used. RTV-2 elastomer are two-component products that, when mixed, cure at room temperature to a solid elastomer, a gel, or a flexible foam. RTV-2 remains flexible from -80C to +250C. Break down occurs at temperatures above 350°C leaving an inert silica deposit that is non-flammable and non-combustible. They can be used for electrical insulation due to their dielectric properties.

The preparation is the same as for hot-press sealing. Every device should be cleaned in ultra-sonic bath with acetone. Input and output holes also should be drilled. Mix RTV-2 (two component) in a 1:10 ratio and then put the mixture into vacuum condition degassing. Usually 40 minutes are sufficient for degassing. A thin glass chip should be attached at the center of a standard glass chip with tape. Use spinner machine to spin RTV mixture on chips and then put them into oven for about 5 minutes at 70C. However this time is very hard to control. The ideal situation is that RTV on chips should be hard but still have some stickiness. If RTV is too cured, the zeonor device can not bond to chips. If RTV is too sticky, it will go into the mixer channels and destroy the structure. Make sure no RTV goes into channels when put zeonor device onto glass chips, then put this stack into oven for 4 hours (longer time is also preferred). After curing, separate the zeonor device with thin glass chip from stack. Because it is really hard to control the time when we pre-heat RTV, usually only one in ten is successful at most.

4.3.2 PDMS device sealing

Plasma cleaner is the most common way to seal PDMS with glass. In our experiment, we tried standard glass chip and PDMS thin film as our cover chip.

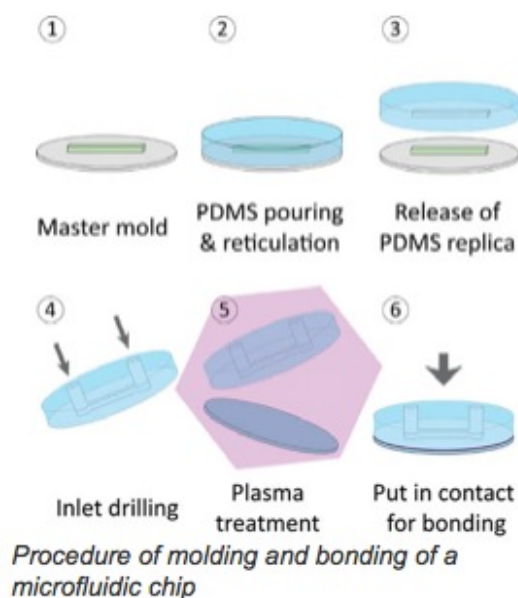


Figure 9. Procedure of molding and bonding a microfluidic chip

Glass chip

Before plasma oxidation, we need to drill the input and output holes at the PDMS, then clean PDMS device and standard glass chip with IPA in ultrasonic bath, then rinse with deionized water, and dry with a stream of nitrogen. Place PDMS channel-side-up on one cover slip, and lay this and a second cover slip in the plasma cleaner. Run the plasma cleaner at high power for about 30 seconds. Remove them from the cleaner and immediately place the second cover slip on the channel side of the PDMS. Press gently and ensure no air pockets form near the channel. The cover slip should bond permanently to the PDMS. Then slowly pry away the unbonded cover slip.

Usually the PDMS bond to glass can hold high pressure. However the maximum flow rate in our samples can only reach 100 ul/min (total flow rate is 200 ul/min) because of the seal between PDMS and tubing.

To improve the seal between PDMS and tubing, we tried several methods.

1. Use metal holder to improve sealing.
2. Use glue to fill the space between PDMS and tubing.
3. Metal holder and glue are both used.

The metal holder we used has a hole at the center that laser can go through. There are four inlet and outlet holes at the sides and every hole also has a rubber o-ring to prevent leaking. A metal cover was used in this holder and we can adjust the pressure to prevent blocking the channel.

In the first method, no glass cover was bonded to PDMS. The holder was also used as the cover to seal PDMS. However, the holder with PDMS was not ideal. Because PDMS is not rigid, it will distort when we screw the metal cover to PDMS. Usually the liquid could not go into the mixer when we do flow experiments. The highest flow rate we recorded with this method is 50 ul/min (total flow rate is 100 ul/min)

In the second method, three straight grooves from the inlet and outlet to the edge were carved before plasma cleaning. After IPA cleaning and plasma cleaner, insert metal tubing into the grooves and then use glue to fill the space between PDMS and tubing. Put mixer in the oven at 70C for 2 hours. It is hard to control the groove depth, sometime it will be too deep and required lots of glue to fill the space. Leaking also

can not be prevented. Usually the flow rate can reach to 100 ul/min (total flow rate is 200 ul/min). The highest flow we recorded is 180 ul/min (total flow rate is 360 ul/min). In the third method, we only drill the inlet and outlet hole before bonding. Use standard glass chip as cover and then put this sandwiched mixer into the holder. The PDMS will not distort because of the glass chip. Use the screws to adjust the pressure. Ensure the channel is not distorted and blocked. With this method, the highest flow rate we recorded is 350 ul/min (total flow rate is 700 ul/min).

4.3.3 Silicon device sealing

Silicon device sealing is similar to zeonor device. Before sealing, the inlet and outlet holes should be drilled, washed with IPA, and then dried with nitrogen. The procedure for RTV sealing for silicon is the same as for zeonor device.

Silicon device is rigid and will not distort with high pressure. So the metal holder we used in zeonor and PDMS devices is ideal for silicon device. Use rubber ring to prevent leaking (no rubber o-ring required in PDMS device sealing) and screw the metal cover down to ensure the mixer will not move.

Another common method to seal silicon device is using PDMS. Because a PDMS thin film is used as the cover and it should not be too soft, the ratio of PDMS monomers and curing agents can be less than 10:1 (we used 7:1 in our experiment). After mixing and degassing, spin PDMS on a thin glass chip and then put chip into the oven at 70C for 4 hours. When PDMS cured, put PDMS chips and silicon into plasma cleaner with

high power for about 20 seconds, then put them together. After bonding a 2-hour bake in the oven at 70°C is recommended.

4.3.4 SU-8 device sealing

An easy and inexpensive method to seal SU-8 device is the adhesive bonding of the SU-8 structures with a cover lid. This is done by applying pressure to the sample while heating above the glass transition temperature (T_g) of the SU-8. Uncrosslinked SU-8 has a glass transition between 50-65C [44]. For crosslinked SU-8 it is known that T_g varies between 150C - 240C depending on the level of crosslinking, which is dependent on the exposure dose and the post exposure bake of the lithographic process [45, 46]. For this particular adhesive bonding process, the level of crosslinked SU-8 should be neither too high, so that SU-8 can still reflow during heating, nor too low, so that the structural quality of SU-8 microstructures is not jeopardized when applying pressure [44]. The simple adhesive bonding is cheaper and simple than anodic, silicon fusion or eutectic bonding, which requires special equipment and cannot be applied to MEMS with polymer structures [47]. Other adhesive bonding methods use additional adhesives, like photosensitive glue. However, these methods require precise dispensing of the glue and very flat sample surfaces. Otherwise, the glue will easily block the channels or the via-holes of the lid.

Another common way to seal SU-8 device is by bonding to PDMS. This method is similar to silicon device bonding to PDMS. Spin PDMS on a thin glass chip, use

plasma cleaner to oxidate PDMS and bond to SU-8. PDMS bond to SU-8 will be easier than the first method we mention above and no clean room condition needed.

5. Flow test and confocal result

5.1 Flow test

Before using confocal microscope to scan, every mixer should be flow tested to ensure the structure of mixer is not distorted. Food dye (blue and red) is used in flow test. In flow test, the food dye should be fresh; otherwise some residues will stay in the channels and break the structure of mixers. Sometimes water also can be used in the flow test to avoid the residue. Two 10ml syringes and two pumps were used in flow test. The flow rate will be changed from low to high to ensure OK, as is the highest flow rate during test. Ensure the two flows are balanced when they meet each other at the junction. We also need an optical microscope to observe the food dye flowing in the channel. No channel block, no leaking and flow force balance are the targets we need to achieve in flow test.

5.2 Confocal microscope

The Leica TCS SP2 confocal microscope is used in our experiment. This confocal microscope is equipped with 458, 478, 488, 514, 543, and 638 nm laser lines for

excitation. The fully spectral system has four fluorescence detectors allowing simultaneous capture of up to 4 colors plus bright field. Real-time sequential acquisition to avoid bleed through or for reflected light confocal (for collagen imaging) is easy to set up. The upright microscope is equipped with high NA oil and water immersion objective and DIC optics.

Cy5 and fluorescein were used as our color dyes. Fluorescein is a fluorophore commonly used in microscope, in a type of dye laser as the gain medium, in forensics and serology to detect latent blood stains, and in dye tracing. Fluorescein has an absorption maximum at 494 nm and emission maximum of 521 nm (in water). Fluorescein also has an isosbestic point (equal absorption for all pH values) at 460 nm. Cy5 is the most popular Cyanine dye. Cy5 is fluorescent in the red region (670 nm) but absorbs in the orange region (650nm). With these two color dyes we can see red and green clearly in confocal tests.

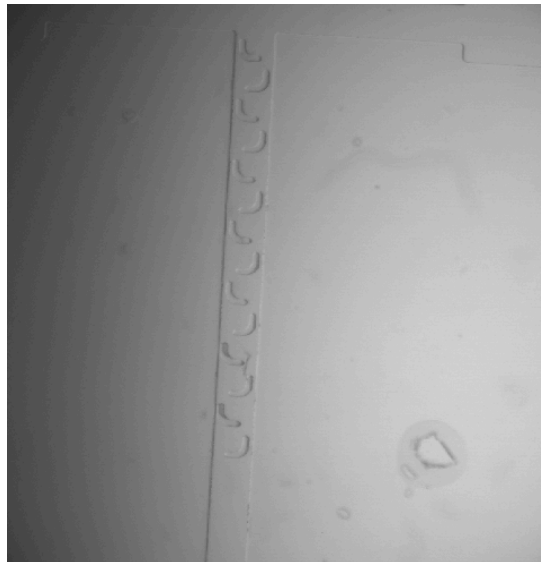
Start Leica Confocal microscope system first and change objective to 10X. Choose fluorescence filter (usually 2 or 3) for viewing in the microscope. Set microscope at bright field mode and then focus on sample. When ready to scan, switch filter to position 4 and pull out knob on upper left of microscope (laser interlock). No images can be viewed from eye lens from now. Check control panel settings at bottom of screen (for the gain-black level knobs). Ensure the gain-black level knobs stay at the lowest level. Also check the objective icon and make sure the one we are using is checked. Usually the objective icon will have right display, but sometimes it does not especially after we change the objective. Hit Continuous to start scanning and adjust

gains and focus until we have a nice image. Set line averaging and use single scan to collect an image, then save it.

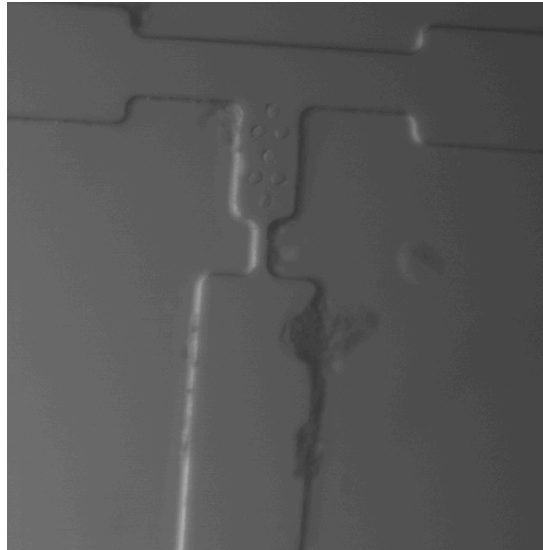
During confocal flow test we use xyz mode to scan mixer from top to bottom. Two pumps are working all the time during the test so we can assume no big flow change will happen in channels as time goes on. The only thing we are concerned about are the movement of the dye in different structures and different depth. The scan speed is 400 MHz (400 lines/s). Sometimes higher speed will be used to get more details (usually 800 MHz and 1000 MHz are used, higher speed will cost more time) .

5.3 Confocal results

Leica Confocal Microscope can show scanning images in different modes at the same time. It also can merge several images to get more information.



(a)



(b)

Figure 10. Images of J-shaped mixer and Pillars mixer in bright field

The structures of channels are distinct. No distortion can be observed in these channels. Some white dots out of channel prove these mixers are sealed well. In fact, these white dots are air bubbles and they are far away from channel edges. No effect will be caused by these bubbles.

J-shaped mixer confocal flow test

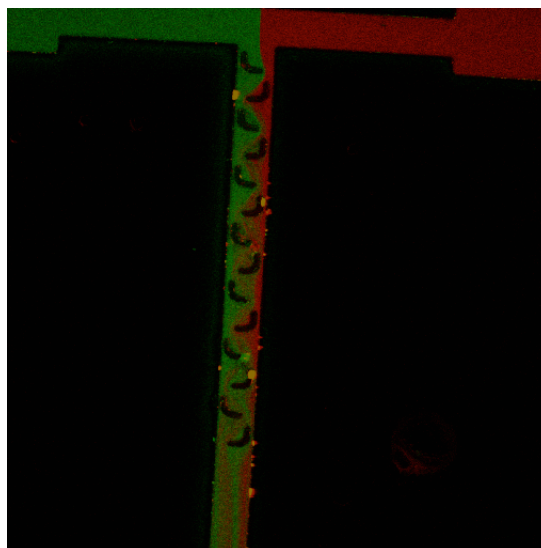
We test J-shaped mixer in different flow rate from 50 ul/min to 200 ul/min (total flow rate is from 100 ul/min to 400 ul/min). However the J-shaped mixer can not hold 200 ul/min for a long time and it will leak.



(a)



(b)



(c)

Figure 11. Single scan of J-shaped mixer with Cy5 and fluorescein. The flow rate for both sides is 100 $\mu\text{l}/\text{min}$. (a) Confocal image only with fluorescein. (b) Confocal image with Cy5. (c) The overview image

There is a distinct interface between red and green and 7 pairs of J shape are also showed in (c). With image (c) we can judge the forces from both sides are equal and the color dye flows along the structure. Distinct black J shapes prove no color dye flow over the features. From (c), we can find two different color dye meet each other at the center of channel and then flow down. The first pair of J shape just split the flow and does not mix two color dyes together. As liquid goes down, green dye goes to right side and red dye goes to left side. These two color dyes mix together at last.

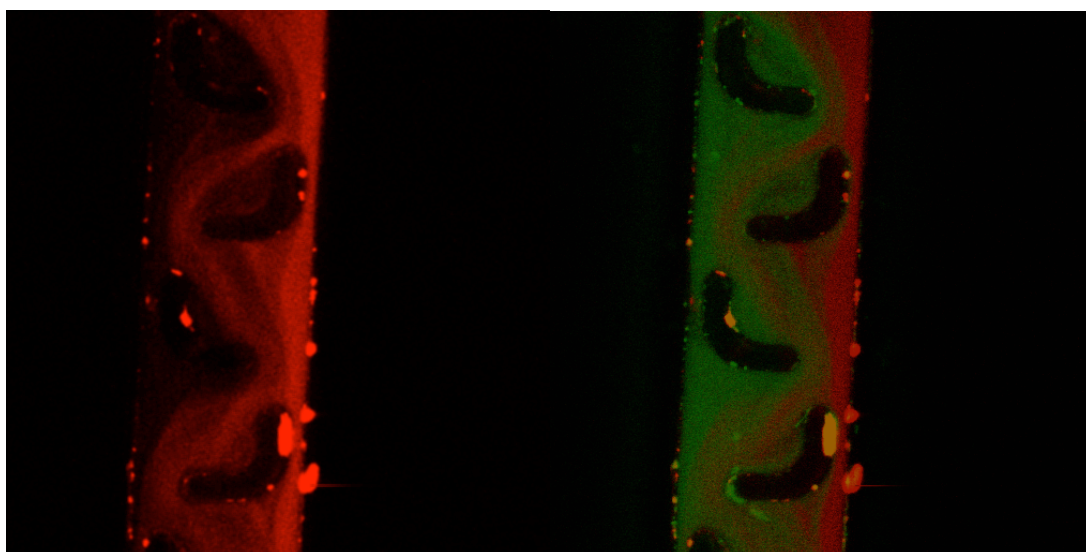
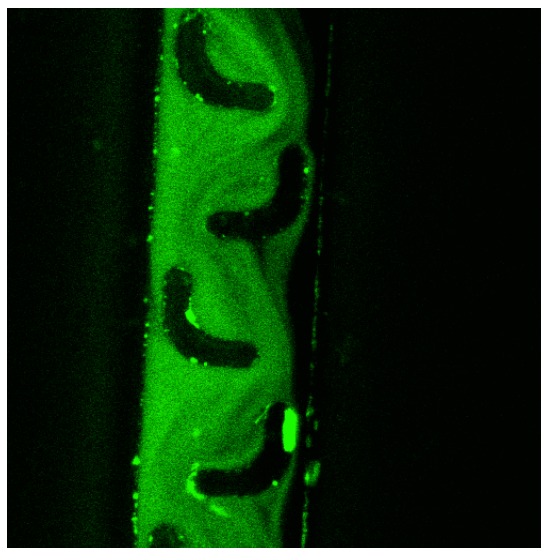
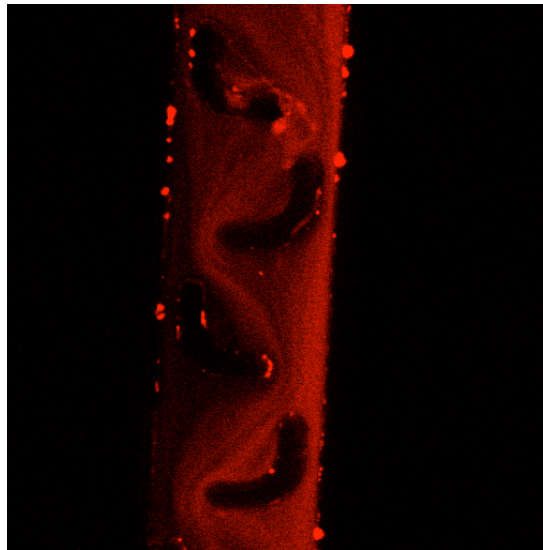
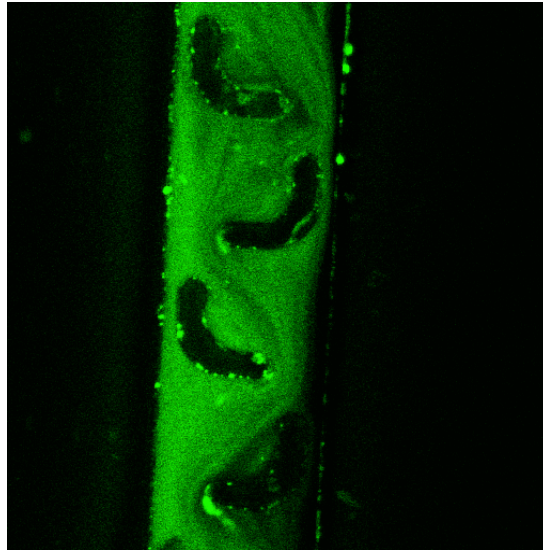


Figure 12. Single scan of second and third pairs of J shape. The flow rate for both sides is 100 $\mu\text{l}/\text{min}$.



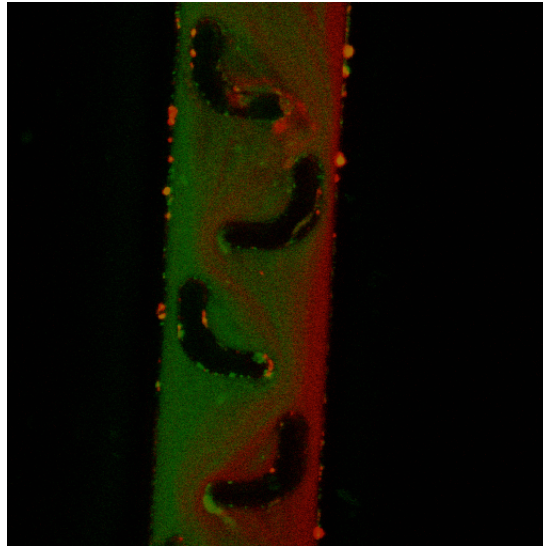
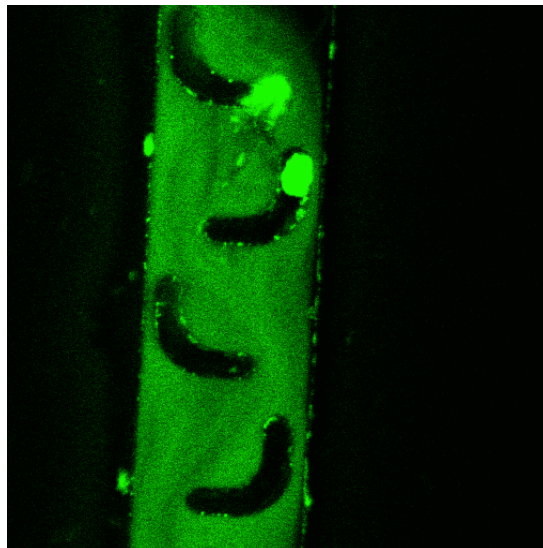


Figure 13. Single scan of fourth and fifth pairs of J shape. The flow rate for both sides is 100 $\mu\text{l}/\text{min}$.



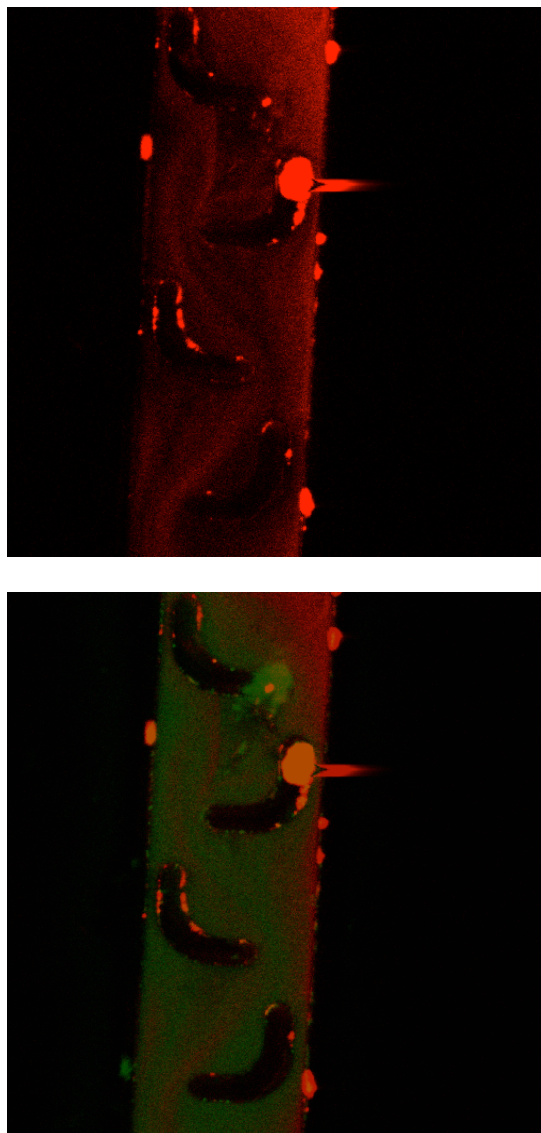
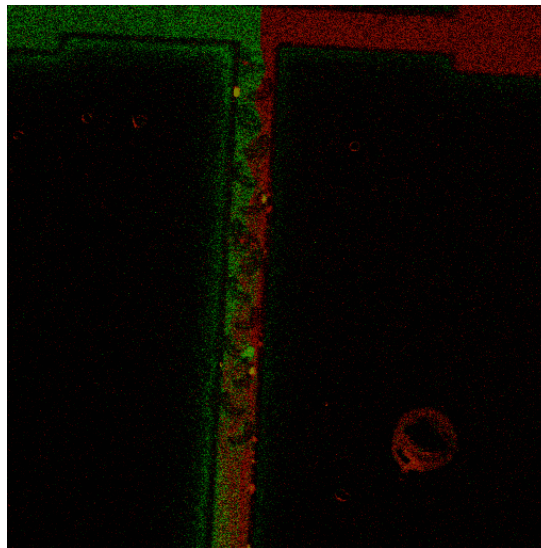


Figure 14. Single scan of sixth and seventh pairs of J shape. The flow rate for both sides is 100 $\mu\text{l}/\text{min}$.

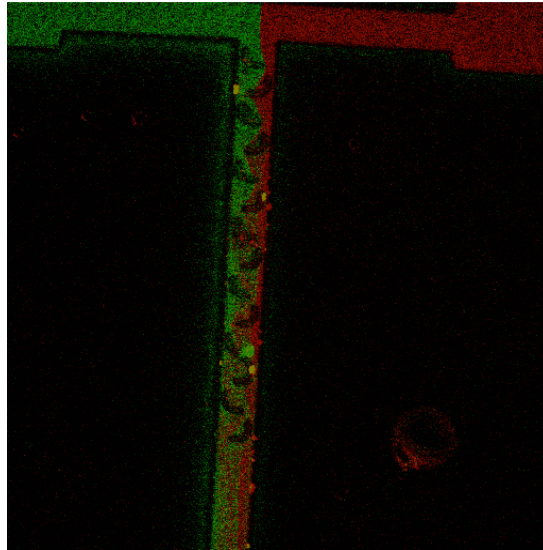
Fig 12 to Fig 14 shows the flow movement at different places along the channel. Mixing begins at the second pairs of J shape and is almost complete at sixth pairs of J shape. Several bright dots are shown in every figure. Maybe these bright dots are

residue of color dye and show strong signals. However every pairs of J shape is complete shape without these bright dots and no damage occurs to these features.

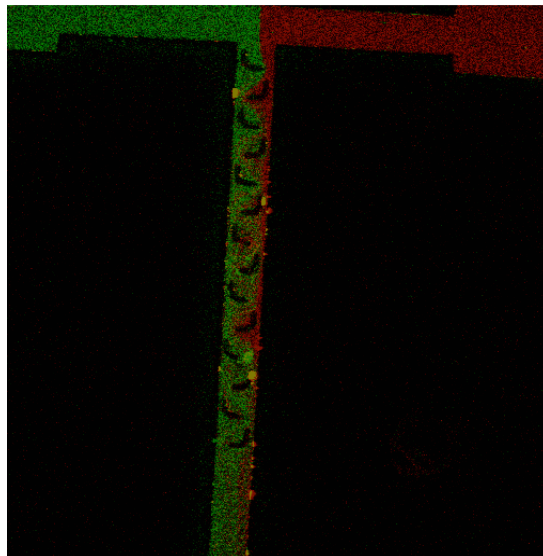
All the figures we mention above are single scan images. In single scan mode, the Leica Confocal Microscope only scans the center of Z direction several times and gets the average. Single scan image does not have any Z direction information.



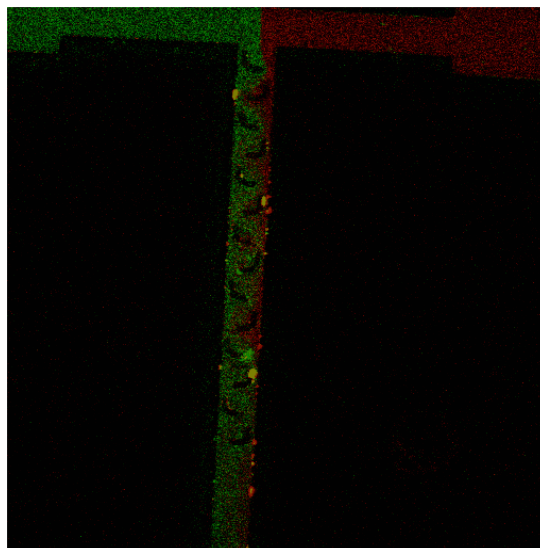
(a)



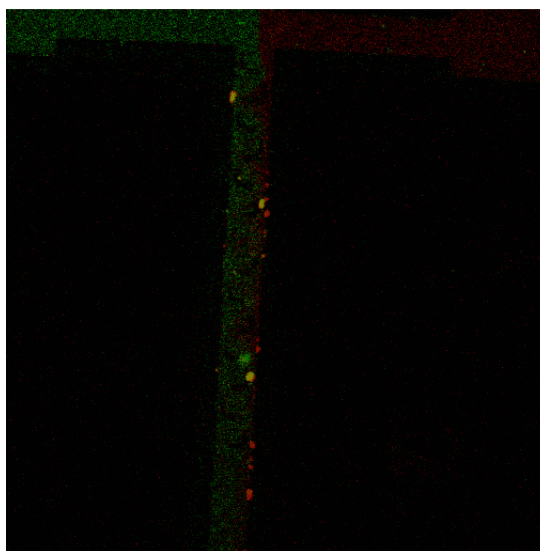
(b)



(c)



(d)



(e)

Figure 15. Confocal image of J-shaped mixer with different depth. Microscope scans from top to bottom and total scan depth is about 58 μm (The depth of channel is about 49.6 μm). The flow rate for both sides is 100 $\mu\text{l}/\text{min}$.

Color dye signals are weak at the top side of mixer, then become stronger as the depth goes down and turn to weak again at the bottom side. In (e), it is hard to find the flow signal expect for several bright dots. In (a) and (b), there is a red ring at the right corner and the small features also has red color, especially the first two pairs.

According to the bright field image, Fig 10 (a), we can judge the red ring is the air bubble. No color dye flow through this air bubble and the bubble only shows red color but no green. We can assume this phenomenon is caused by PDMS excitation. So the red color on small features is also caused by PDMS excitation, not the dye flowing over features. Those Z depth scan image are similar to the single scan image. From this we can judge there is little or even no flow movement at the Z direction and the mixing effect is only cause by the J-shaped structures.

Pillars mixer confocal flow test

We test the pillar mixer under different flow rate from 50 ul/min to 200 ul/min (total flow rate is from 100 ul/min to 400 ul/min). However, 150 ul/min is the highest flow rate we can achieve. Above 150 ul/min, the mixer will leak.

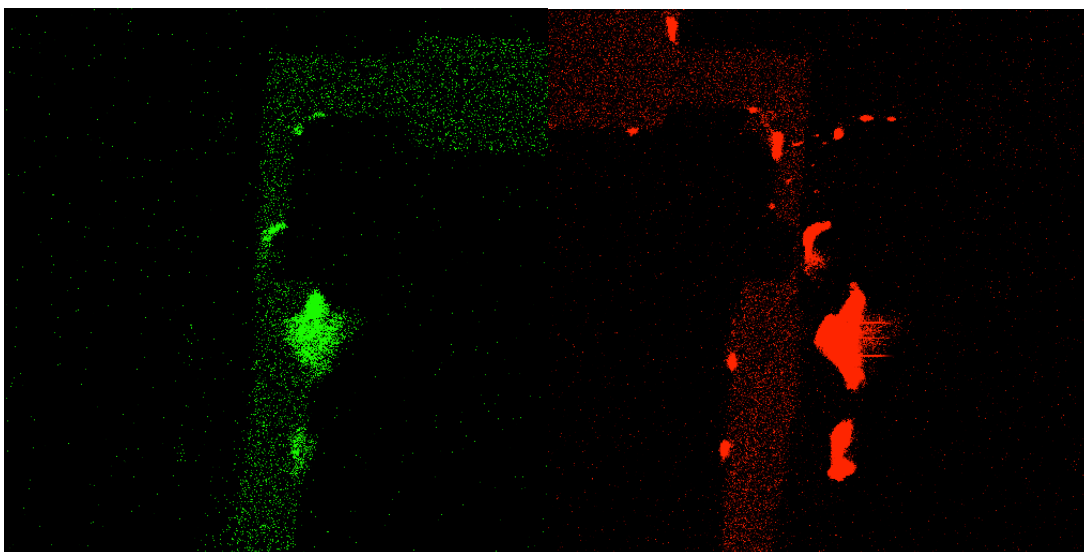


Figure 16. Single scan image of pillars mixer. The flow rate for both sides is 50 ul/min

In single scan image of the pillar mixer, there is a really big bright dot and it shows both green and red. According to the bright field image, figure 10 (b), we think these dots are some residue of Cy5 and fluorescein. Two color dyes meet each other at the center of channel but flow parallel for a very long distance. At the bottom of these two images, we can see only a little fluorescein move to left. This phenomenon is caused by diffusion, not pillars. Another problem we can find from Fig 16, no pillars shadow is displayed. However we can find seven vertical pillars in the bright field images (Fig 10). Z direction scan and increasing flow rate (Fig 17) were also applied to this pillar mixer, but no pillars shadow was found. This mixer sample was made by PDMS and bonded to the glass chip. Probably the most likely reason is that these pillars are very short and can not reach to the glass cover. The broken structure does not have mixing function.

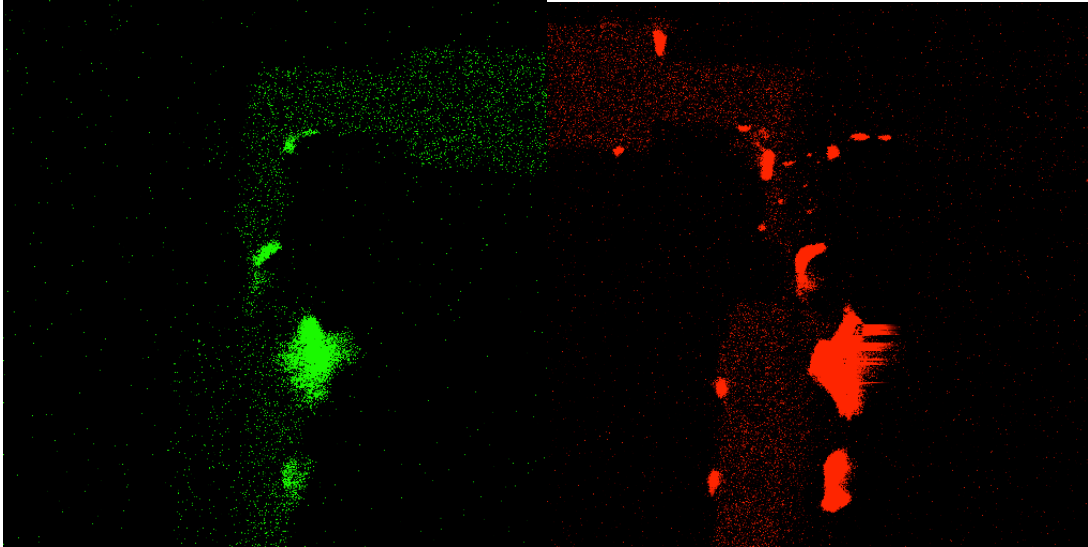


Figure 17. Single scan image of pillars mixer. The flow rate for both sides is 120
ul/min

PDMS is not a good material to fabricate such a mixer with very small features (the diameter of pillars in our experiment is 10 μm , height is 50 μm). When PDMS is released from the master, the small vertical pillars will broke easily. According to this reason, we try to use silicon and SU-8 to fabricate this kind mixer.

6.Calculation

Mixing time

In Fig 11, two color dyes have complete mixing at the end of seven pairs of J shape.

We can calculate the mixing time with the mixer parameters and flow rate.

Flow rate in Fig 11 is 100 ul/min for both sides. The width of channel is 100um and depth is 50um. The total distance that color dyes flow through is 1120um (7 pairs of J shape length). Mixing time equals the total volume divide by the flow rate. After calculation we get the mixing time is about 1.4ms. Another important parameter is Reynolds number. For Cy5 and fluorescein, the Re number is about 67 with 100 ul/min flow rate. However we can increase the flow rate and the highest flow rate we achieved is 350 ul/min for both sides. As flow rate goes up, the mixing time will goes down. The shortest mixing time is about 400us. This mixing time shows this J-shaped mixer has a good function on mixing liquid. Normally, the Tee type mixer has a 10-100 ms mixing time.

Mixing efficiency

The percentage of mixing can be determined by the following equation:

$$\phi = (1 - \sigma/\sigma_0) \times 100$$

Where σ is the standard deviation, and the subscript o represents the initial unmixed state in the mixer.

$$\sigma = \sqrt{\frac{1}{N-1} \sum_{i=1}^N (X_i - \bar{X}_i)^2}$$

$$\bar{X}_i = \frac{\sum_{i=1}^N X_i}{N}$$

In this equation σ is the standard deviation, X_i and \bar{X}_i are the concentration at the measured points and the mean value in the main channel, respectively.

In Lin's paper [49], they shows the simulated mixing performance with posts number at $Re = 5, 20, 50, 150,$ and $350,$ respectively. The percentage of mixing increased as the number of posts increased. At the same number of posts, the percentage of mixing at a higher Reynolds number was larger.

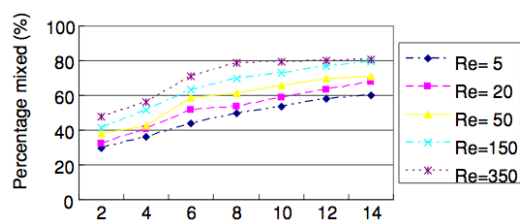


Figure 18. Mixing percentage in the Tee channel with J-shaped calculated from simulated results.

In our experiment, the Re number is 67 and the number of J-shaped posts is 14 . The mixing percentage based on experiment data is about 72% , a little lower than the simulated results.

7 Conclusions

This study tests and verifies two novel designs of passive microfluidic mixer. One has several J-shaped baffles in the main channel to enhance mixing; the other has several vertical pillars posts. The mixing performance of J-shaped mixer is really good with PDMS material, while vertical pillars do not work well. According to the fabrication, we can find Zeonor and PDMS are best suited to fabricate micromixer with large

features. In other aspects, these two materials are cheap and the master can be re-used many times. Silicon and SU-8 can be used to fabricate micromixer with small features. Because of the rigidity of silicon, the small features, like the vertical pillars in our experiment, will not be easily broken. The down side of these two devices is that the material is expensive. How to improve the sealing effect is still a problem in our experiment. Higher flow rate could have short mixing time, bigger Re number and better mixing. However there is a limitation in flow rate for micromixer, especially for PDMS device. Too high flow rates will distort the structure of channel or even break mixers.

The future work we should concern about is that:

1. Improve sealing effect and reduce the leaking phenomenon.
2. Try to make several Zeonor device. Do not break the structure of channel when using hot plate or find some other tools can imprint small features with low temperature.

REFERENCES

1. Kakuta M, Bessoth F G and Manz A 2001 Microfabricated devices for fluid mixing and their application for chemical synthesis *Chem. Rec.* **1** 395–405
2. Reyes D R et al 2002 Micro total analysis systems: 1. Introduction, theory, and technology *Anal. Chem.* **74** 2623–36
3. Vilckner T et al 2004 Micro total analysis systems. Recent developments *Anal. Chem.* **76** 3373–86
4. Erbacher C et al 1999 Towards integrated continuous-flow chemical reactors *Mikrochim. Acta* **131** 19–24
5. Hinsmann P et al 2001 Design, simulation and application of a new micromixing device for time resolved infrared spectroscopy of chemical reactions in solutions *Lab on a Chip* **1** 16–21
6. Veenstra T T 1999 Characterization method for a new diffusion mixer applicable in micro flow injection analysis systems *J. Micromech. Microeng.* **9** 199–202
7. Kakuta M et al 2003 Micromixer-based time-resolved NMR: applications to ubiquitin protein conformation *Anal. Chem.* **75** 956–60
8. Lin Y et al 2003 Ultrafast microfluidic mixer and freeze–quenching device *Anal. Chem.* **75** 5381–6
9. Haverkamp V et al 1999 the potential of micromixers for contacting of disperse liquid phases *Fresenius' J. Anal. Chem.* **364** 617–24
10. Dertinger S K W et al 2001 Generation of gradients having complex shapes using microfluidic networks *Anal. Chem.* **73** 1240–6
11. Lin Y C et al 2007 Mixing enhancement of the passive microfluidic mixer with J-shaped baffles in the tee channel *Biomed Microdevices* **9** 215–221
12. Yi M and Bau H H 2003 The kinematics of bend-induced mixing in micro-conduits *Int. J. Heat Fluid Flow* **24** 645–56
13. Knight J B, Vishwanath A, Brody J P and Austin R H 1998 Hydrodynamic focusing on a silicon chip: mixing nanoliters in microseconds *Phys. Rev. Lett.* **80** 3863–6

14. Hye Yoon Park et al 2006 Achieving uniform mixing in a microfluidic device: Hydrodynamic focusing prior to mixing *Anal. Chem.* **78** 4465-4473
15. Johnson T J, Ross D and Locascio L E 2002 Rapid microfluidic mixing *Anal. Chem.* **74** 45-51
16. Branebjerg J et al 1996 Fast mixing by lamination Proc. *MEMS'96, 9th IEEE Int. Workshop Micro Electromechanical System* (San Diego, CA) pp 441-6
17. Schwesinger N et al 1996 A modular microfluid system with an integrated micromixer *J. Micromech. Microeng.* **6** 99-102
18. Deshmukh A A, Liepmann D and Pisano A P 2000 Continuous micromixer with pulsatile micropumps *Technical Digest of the IEEE Solid State Sensor and Actuator Workshop* (Hilton Head Island, SC) pp 73-6
19. Niu X Z and Lee Y K 2003 Efficient spatial-temporal chaotic mixing in microchannels *J. Micromech. Microeng.* **13** 454-62
20. Deval J, Tabeling P and Ho C M 2002 A dielectrophoretic chaotic mixer Proc. *MEMS'02, 15th IEEE Int. Workshop Micro Electromechanical System* (Las Vegas, Nevada) pp 36-9
21. Jacobson S C, McKnight T E and Ramsey J M 1999 Microfluidic devices for electrokinematically driven parallel and serial mixing *Anal. Chem.* **71** 4455-9
22. Tang Z et al 2002 Electrokinetic flow control for composition modulation in a microchannel *J. Micromech. Microeng.* **12** 870-7
23. Bau H H, Zhong J and Yi M 2001 A minute magneto hydro dynamic (MHD) mixer *Sensors Actuators B* **79** 207-15
24. Moroney R M, White R M and Howe R T 1991 Ultrasonically induced microtransport Proc. *MEMS'91, 3th IEEE Int. Workshop Micro Electromechanical System* (Nara, Japan) pp 277-82
25. Zhu X and Kim E S 1997 Acoustic-wave liquid mixer *Microelectromechanical Systems (MEMS) American Society of Mechanical Engineers, Dynamic Systems and Control Division (Publication) DSC vol 62* (ASME, Fairfield, NJ, USA) pp 35-8
26. Mao H, Yang T and Cremer P S 2002 A microfluidic device with a linear temperature gradient for parallel and combinatorial measurements *J. Am. Chem. Soc.* **124** 4432-5

27. Woias P 2004 Micropumps-past, progress and future prospects *Sensors Actuators B* at press
28. Yasuda K 2000 Non-destructive, non-contact handling method for biomaterials in micro-chamber by ultrasound *Sensors Actuators B* **64** 128–35
29. Hosokawa K, Fujii T and Endo I 1999 Droplet-based nano/picoliter mixer using hydrophobic microcapillary vent *Proc the IEEE International Workshop Micro Electromechanical System (Piscataway, NJ, USA)* pp 388–93
30. Stokes, George (1851). "On the Effect of the Internal Friction of Fluids on the Motion of Pendulums". *Transactions of the Cambridge Philosophical Society* **9**: 8–106. Bibcode 1851TCaPS...9....8S
31. Reynolds Number Engineeringtoolbox.com
32. Holman, J. P.. *Heat Transfer*. McGraw Hill
33. See e.g. Hessel et al., 2003
34. Duffy D, McDonald J, Schueller O and Whitesides G 1998 Rapid prototyping of microfluidic systems in poly(dimethylsiloxane) *Anal. Chem.* **70** 4974–84
35. Hong C C, Choi J W and Ahn C H 2004 A novel in-plane microfluidic mixer with modified tesla structures *Lab on a Chip* **4** 109–13
36. Munson M S and Yager P 2004 Simple quantitative optical method for monitoring the extent of mixing applied to a novel microfluidic mixer *Anal. Chim. Acta* **507** 63–71
37. "Linear Polydimethylsiloxanes" Joint Assessment of Commodity Chemicals, September 1994 (Report No. 26) ISSN 0773-6339-26
38. McDonald, J. C.*et al.* (2000). "Fabrication of microfluidic systems in poly(dimethylsiloxane)". *Electrophoresis* **21** (1): 27–40.
39. "Semi" SemiSource 2006: A supplement to Semiconductor International. December 2005. Reference Section: *How to Make a Chip*. Adapted from Design News. Reed Electronics Group.
40. Levy, Roland Albert (1989). *Microelectronic Materials and Processes*. pp. 1–2. ISBN 0-7923-0154-4. Retrieved 2008-02-23.
41. Grovenor, C. (1989). *Microelectronic Materials*. CRC Press. pp. 113–123. ISBN 0-85274-270-3. Retrieved 2008-02-25.

42. Liu, J.; Cai, B.; Zhu, J.; Ding, G.; Zhao, X.; Yang, C.; Chen, D. "Process research of high aspect ratio microstructure using SU-8 resist" *Microsystem Technologies* 2004, V10, (4), 265.
43. Jesse Greener, Wei Li, Judy Ren, Dan Voicu, Viktoriya Pakhareno, Tian Tang and Eugenia Kumacheva "Rapid, cost-efficient fabrication of microfluidic reactors in thermoplastic polymers by combining photolithography and hot embossing" *Lab Chip*, 2010
44. Blanco F J, Agirregabiria M, Garcia J et al. Novel three-dimensional embedded SU-8 microchannels fabricated using a low temperature full wafer adhesive bonding. *J. Micromech. Microeng.* 14 (2004), 1047–1056.
45. Song Y, Kumar C S S R, Hormes J et al. Fabrication of an SU-8 based microfluidic reactor on a PEEK substrate sealed by a ‘flexible semi-solid transfer’(FST) process. *J. Micromech. Microeng.* 14 (2004) 932–940.
46. Feng R, Farris R J. Influence of processing conditions on the thermal and mechanical properties of SU8 negative photoresist coatings. *J. Micromech. Microeng.* 13 (2003) 80–88.
47. Madou M *Fundamentals of microfabrication. The science of miniaturization.* 2nd edition, CRC PressLLC, (2002).